

Modeling and dynamical analysis of a COVID-19 epidemic model with time-delay

Abdul Hussain Surosh¹, Reza Khoshsiar Ghaziani² and Javad Alidousti²

¹ Department of Mathematics, Baghlan University, Pol-e-Khomri, Baghlan, Afghanistan

² Department of Applied Mathematics, Shahrekord University, Shahrekord, P.O.Box 115, Iran

ABSTRACT. In this paper, the local stability of the endemic equilibrium and existence of a Hopf bifurcation in a Susceptible-Exposed-Infected-Recovered (SEIR) delayed mathematical model for COVID-19 pandemic are investigated. By using time-delay as a bifurcation parameter, the associated characteristic equation is analyzed to reveal dynamics of the model. Finally, numerical simulations are performed with suitable parameters choice to illustrate the theoretical results of the model.

Keywords: COVID-19 epidemic model, Time-delay, Stability, Hopf bifurcation, SEIR model.

2000 Mathematics subject classification: 34K18, 34K20; Secondary 92C10, 95C15.

1. INTRODUCTION

Coronavirus disease 2019 (COVID-19) is an infectious disease that can cause illnesses range from the common cold to much more severe illnesses like SARS and MERS [3]. This type of diseases which has an enormous impact on the

¹Corresponding author: surosh_272@yahoo.com


Received: 13 April 2023

Revised: 10 October 2023

Accepted: 12 October 2023

How to Cite: Surosh, Abdul Hussain; Khoshsiar Ghaziani, Reza; Alidousti, Javad. Modeling and dynamical behavior of an SEIR Type COVID-19 pandemic model with time-delay, *Casp.J. Math. Sci.*, **12**(2)(2023), 363-377.

This work is licensed under a Creative Commons Attribution 4.0 International License.

 Copyright © 2023 by University of Mazandaran. Submitted for possible open access publication under the terms and conditions of the Creative Commons Attribution(CC BY) license(<https://creativecommons.org/licenses/by/4.0/>)

world population and economy, emerged as a sudden pandemic disease within human population and has become a worldwide emergency [20, 4, 8]. Many scientists and researchers have combined efforts in order to develop several approaches for understanding the COVID-19 transmission dynamics and find out the effective control ways for preventing the virus spreads [4, 3]. Mathematical modeling is recognized as an essential tool for understanding the transmission dynamics of HIV/AIDS as well as COVID-19 pandemic. Since the last decades, the direct implementation of a mathematical model in epidemiology has proven to be helpful in further understanding the dynamics of infectious diseases and the corresponding control problems [1, 4, 14]. Therefore, mathematical models play a vital role in analyzing the mechanism of spread and control of infectious diseases such as COVID-19 in the human population [21, 7].

Several epidemic models, with various characteristics, have been described and investigated in the literature. Most of these models are based on the SIR and SEIR framework and its simple variations [18, 13]. Amongst the various diseases models, Susceptible-Exposed-Infectious-Removed (SEIR) mathematical epidemic model has been a widely used and accepted model for distinguishing the outbreak of the COVID-19 epidemic in different regions of the world [22, 5]. Indeed, the SEIR model is a widely utilized model which can show the progressions of individuals between four different states: Susceptible (S) (an individual is Susceptible to catch the disease and hence the population is not resistant to illness), Exposed (E) (an individual or population fraction is infected with the virus but does not transmit to others, because the disease is in the incubation period), Infectious (I) (an individual is Infective, this means that one who has got the disease and is able to infect others), and Recovered (R) (an individual has Recovered from infection and is immune from further infection). Therefore, in the generic SEIR model, an individual is able to only move from compartment S to E , from compartment E to I , and then from compartment I to R [15, 12, 5].

There is another important factor, namely, time-delay which its introduction to mathematical epidemic models has been studied in order to better understand and describe the transmission dynamics of infectious diseases [26]. Moreover, time delay is ubiquitous in most biological systems like predator-prey models and epidemiological models. In fact, inclusion of delays in epidemic models makes them more realistic and can reflect the real dynamical behaviors of models that depend also on the past history of systems [1, 19]. Time-delay, which happens usually due to system process and information flow in a particular part of dynamical systems, is considered as a natural element of the dynamic process of economics, biology, epidemiology, ecology, mechanics and physiology [10, 16].

Recently, time-delayed differential equations have been utilized in modeling the spread of COVID-19. It was used to describe the characteristics of COVID-19, such as incubation and latent period, recovery time, diagnosis time, and immune response [2]. For instance, Gao et al. [9] formulated an SEIR epidemic model with two time-delays and pulse vaccination for studying the control of spread and transmission of an infectious disease. Tipsri and Chinviriyasit [17] investigated the effect of time-delay on the stability of bifurcating periodic solutions and direction of Hopf bifurcation of an SEIR model with nonlinear incidence. Cakan, in [6] proposed an SEIR model representing the latent period of COVID-19 as a time-delay parameter. The model investigates the capacity of health care by assuming the variability of recovery and death rates due to COVID-19. Radha and Balamuralitharan [15] considered the time-delay for the immune system to respond to the transmission dynamics of COVID-19. Yang and Zhang [23] described the propagation dynamics of COVID-19 using the SEIQR model with two time-delays. They considered the delay in time for an exposed individual to convert to an infected individual. They also incorporated time-delay in the model recovery for exposed, infected, and quarantined individuals.

Moreover, Lu et al. [11] presented an SIQR model with a time-delay from infection to recovery. The influence of the time-delay from infection to recovery was discussed in detail. According to their conclusions, when the time-delay from infection to isolation be smaller, the COVID-19 epidemic is better controlled.

Motivated by the early research and since the stability and bifurcation have great significance to epidemic models, and time-delay also has a considerable influence on the virus spread and its control, thus, we attempt to explore the effect of time-delay on the dynamics of COVID-19 epidemic model and analyze the stability and Hopf bifurcation phenomena. Hence in this work, we consider a system of ODE which are formulated in [3] and has the following form:

$$\begin{cases} \dot{S}(t) = \eta + \rho R(t) - \alpha S(t)I(t) - \delta S(t) - \mu S(t), \\ \dot{E}(t) = \alpha S(t)I(t) - \beta E(t) - \delta E(t) - \mu E(t), \\ \dot{I}(t) = \beta E(t) - \gamma I(t) - \delta I(t) - \mu I(t), \\ \dot{R}(t) = \gamma I(t) - \rho R(t) - \delta R(t) - \mu R(t), \end{cases} \tag{1.1}$$

where $\lambda(t) = I(t)$ shows the force of infection and the initial conditions are considered as follows:

$$S(0) > 0, E(0) > 0, I(0) > 0, R(0) > 0.$$

By following [24, 25] and incorporating of time-delay in (1.1), we formulate and introduce the following COVID-19 epidemic model:

$$\begin{cases} \dot{S}(t) = \eta + \rho R(t) - \alpha S(t)I(t) - a_1 S(t), \\ \dot{E}(t) = \alpha S(t)I(t) - a_2 E(t), \\ \dot{I}(t) = \beta E(t) - \gamma I(t - \tau) - a_3 I(t), \\ \dot{R}(t) = \gamma I(t - \tau) - a_4 R(t), \end{cases} \quad (1.2)$$

where $a_1 = a_3 = \delta + \mu$, $a_2 = \beta + a_1$, $a_4 = \rho + a_1$ and the time-delay τ represents the duration from infection to recovery process. The total population size is set as N , i.e, $S(t) + E(t) + I(t) + R(t) = N$ and hypotheses of the model with description of model parameters which are shown in Table 1 can be found in [3].

TABLE 1. Description of the model parameters.

| Parameter | Description |
|-----------|---|
| η | Constant influx of new susceptible. With this rate new susceptible class will Recruited and will enter into susceptible class |
| α | Infection rate or Contact rate or effective contact rate. With this rate covid-19 transfer from compartment S to E |
| β | Latency transfer rate. With this rate exposed class moves from compartment E to compartment I |
| γ | Recovery rate or removal rate. With this rate infected class moves from compartment E to R |
| ρ | Loss immunity (re-infection rate). With this rate recovered class moves from compartment R to S |
| δ | Death rate due to infection of COVID-19. With this rate all class of compartment suffer due to the diseases |
| μ | Natural death rate. With this rate all class of Compartment suffer natural death rate. |

The main objective of this paper includes exploring the effect of time-delay in the COVID-19 epidemic model by analyzing the stability of the model and the existence of Hopf bifurcation. The rest of the paper is organized as follows. In Section 3, we focus on the theoretical results, i.e, stability and Hopf bifurcation phenomena by analyzing of the roots of characteristic equation of the delayed model. We also analyze the existence and stability of the endemic equilibrium point and the existence of Hopf bifurcation. We further calculate the critical time-delay from infection to recuperation and analyze the dynamic properties of the considered time-delayed model. In Section 4, we proceed to present the results of some numerical simulations to verify the correctness of the discussed theoretical analysis. Finally, a brief conclusion is performed in Section 5.

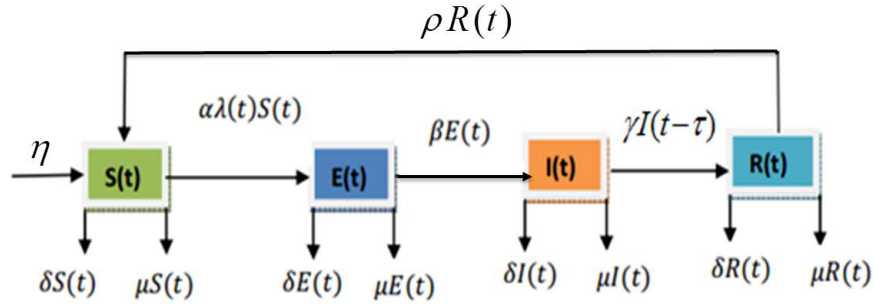


FIGURE 1. State transition diagram of the pandemic model (1.2).

2. POSITIVITY AND BOUNDEDNESS PROPERTIES OF THE MODEL

To study the positivity and boundedness phenomena for the solution of system (1.2), we prove if $S(0) \geq 0, E(0) \geq 0, I(0) \geq 0, R(0) \geq 0$, the solution $S^*(t), E^*(t), I^*(t), R^*(t)$ for system (1.2) is positive when $\tau = 0$. It is not an easy task to prove that the solution of time-delay system (1.2) is positive when $\tau > 0$. However, according to our numerical simulation, we can obtain that when system (1.2) is stable, the solution of system (1.2) is always positive, which is not contradictory to the positivity of the solution to system (1.2). Now we present the following theorem for $\tau = 0$.

Theorem 2.1. *If $S(0) \geq 0, E(0) \geq 0, I(0) \geq 0, R(0) \geq 0$, the solution $S^*(t), E^*(t), I^*(t), R^*(t)$ of the time-delayed model (1.2) is nonnegative and bounded when $\tau > 0$.*

Proof. Here we first prove that $S^*(t) \geq 0$ when $t \geq 0$ based on the initial condition of time-delayed model (1.2). We suppose that $S^*(t)$ is not always nonnegative for $t \geq 0$ and make t_1 to represent the first time that $S^*(t_1) = 0$ and $S'(t_1) < 0$. Based on the first equation of time-delayed model (1.2), we can get $S'(t_1) = \eta > 0$. The two conclusions we obtain are contradictory. Hence, $S^*(t) \geq 0$ when $t > 0$. In similar way, $E^*(t) \geq 0, I^*(t) \geq 0, R^*(t) \geq 0$ when $t > 0$. This implies that when $t > 0$, the solution of system (1.2) is positive. Since $N(t) = S(t) + E(t) + I(t) + R(t)$, where $N(t)$ represent the total size of population at time t . $N'(t) = \eta - (\delta + \mu)(S(t) + I(t)) - a_1(E(t) - R(t))$. Then, we can obtain $\limsup_{t \rightarrow \infty} N(t) = \frac{\eta}{\delta + \mu}$. Hence, the solution $S^*(t), E^*(t), I^*(t), R^*(t)$ of the delayed system (1.2) is bounded when $t > 0$. □

3. STABILITY AND HOPF BIFURCATION ANALYSIS

In this section, we analyze the local stability of positive or endemic equilibrium point and the existence of Hopf bifurcation. It is not difficult to verify

under the condition

$$(\mathbf{H}_1) \quad \begin{cases} \alpha\beta > 0, \\ \gamma + a_3 > 0, \\ a_1a_2(\gamma + a_3) > \alpha\beta\eta, \\ a_2a_4(\gamma + a_3) < \gamma\beta\rho, \end{cases}$$

the delayed model (1.2) has a unique positive equilibrium point

$$E^\star(S^\star, E^\star, I^\star, R^\star),$$

where

$$S^\star = \frac{(\gamma + a_3)a_2}{\alpha\beta}, \quad E^\star = -\frac{a_4(-a_1(\gamma + a_3)a_2 + \alpha\beta\eta)(\gamma + a_3)}{\alpha\beta(-a_4(\gamma + a_3)a_2 + \rho\beta\gamma)},$$

$$I^\star = -\frac{a_4(-a_1(\gamma + a_3)a_2 + \alpha\beta\eta)}{\alpha(-a_4(\gamma + a_3)a_2 + \rho\beta\gamma)}, \quad R^\star = -\frac{(-a_1(\gamma + a_3)a_2 + \alpha\beta\eta)\gamma}{\alpha(-a_4(\gamma + a_3)a_2 + \rho\beta\gamma)}.$$

In order to transfer the equilibrium point to the origin and to linearize the delayed system around it, we use the linear transformation $V_1(t) = S(t) - S^\star$, $V_2(t) = E(t) - E^\star$, $V_3(t) = I(t) - I^\star$ and $V_4(t) = R(t) - R^\star$. Then, by applying the Taylor series expansion at E^\star around the origin, we obtain

$$\begin{cases} \dot{S}(t) = (-a_1 + \alpha I^\star)V_1(t) - \alpha S^\star V_3(t) + \rho V_4(t) - \alpha V_1(t)V_3(t), \\ \dot{E}(t) = \alpha I^\star V_1(t) - a_2 V_2(t) + \alpha S^\star V_3(t) + \alpha V_1(t)V_3(t), \\ \dot{I}(t) = \beta V_2(t) - \gamma V_3(t - \tau) - a_3 V_3(t), \\ \dot{R}(t) = \gamma V_3(t - \tau) - a_4 V_4(t), \end{cases} \quad (3.1)$$

where its linear part can be written as

$$\frac{dV}{dt} = G_1 V(t) + G_2 V(t - \tau), \quad (3.2)$$

in which

$$V(t) = \begin{bmatrix} V_1(t) \\ V_2(t) \\ V_3(t) \\ V_4(t) \end{bmatrix}, \quad G_1 = \begin{bmatrix} -a_1 - \alpha I^\star & 0 & -\alpha S^\star & \rho \\ \alpha I^\star & -a_2 & \alpha S^\star & 0 \\ 0 & \beta & -a_3 & 0 \\ 0 & 0 & 0 & -a_4 \end{bmatrix},$$

$$G_2 = \begin{bmatrix} 0 & 0 & 0 & 0 \\ 0 & 0 & 0 & 0 \\ 0 & 0 & -\gamma e^{-\lambda\tau} & 0 \\ 0 & 0 & \gamma e^{-\lambda\tau} & 0 \end{bmatrix}.$$

Let

$$\begin{aligned}
 m_3 &= \alpha I^* + a_1 + a_2 + a_3 + a_4, \\
 m_2 &= a_4(\alpha I^* + a_1 + a_2 + a_3) + (\alpha I^* + a_1 + a_3)a_2 + (a_3 I^* - \beta S^*)\alpha \\
 &\quad + a_1 a_3, \\
 m_1 &= a_4[(\alpha I^* + a_1 + a_3)a_2 + (a_3 I^* - \beta S^*)\alpha + a_1 a_3] + (\alpha I^* + a_1)a_2 a_3 \\
 &\quad - a_1 \alpha \beta S^*, \\
 m_0 &= a_4(a_2 a_3(\alpha I^* + a_1) - \alpha \beta S^*), \quad h_3 = \gamma, \quad h_2 = \gamma(\alpha I^* + a_1 + a_2 + a_4), \\
 h_1 &= \gamma[(\alpha I^* + a_1 + a_2)a_4 + (\alpha I^* + a_1)a_2], \\
 h_0 &= \gamma[a_2(\alpha I^* + a_1)a_4 + \alpha \beta \rho I^*].
 \end{aligned}$$

Then the characteristic equation of the linearized system can be obtained as

$$\Delta(\lambda, \tau) = Q_1(\lambda) + Q_2(\lambda)e^{-\lambda\tau} = 0, \tag{3.3}$$

where

$$\begin{aligned}
 Q_1(\lambda) &= \lambda^4 + m_3\lambda^3 + m_2\lambda^2 + m_1\lambda + m_0, \\
 Q_2(\lambda) &= h_3\lambda^3 + h_2\lambda^2 + h_1\lambda + h_0.
 \end{aligned}$$

When $\tau = 0$, the characteristic polynomial (3.3) becomes

$$\lambda^4 + (m_3 + h_3)\lambda^3 + (m_2 + h_2)\lambda^2 + (m_1 + h_1)\lambda + m_0 + h_0 = 0. \tag{3.4}$$

By the helps of Routh-Hurwitz criterion, we can find out the sufficient conditions which states that all the roots (3.4) have negative real parts. These conditions have the following form:

$$(\mathbf{H}_2) \quad \left\{ \begin{aligned}
 \Delta_1 &= m_3 + h_3 > 0, \\
 \Delta_2 &= \begin{vmatrix} m_3 + h_3 & 1 \\ m_1 + h_1 & m_2 + h_2 \end{vmatrix} > 0, \\
 \Delta_3 &= \begin{vmatrix} m_3 + h_3 & 1 & 0 \\ m_1 + h_1 & m_2 + h_2 & m_3 + h_3 \\ 0 & m_0 + h_0 & m_1 + h_1 \end{vmatrix} > 0, \\
 \Delta_4 &= \begin{vmatrix} m_3 + h_3 & 1 & 0 & 0 \\ m_1 + h_1 & m_2 + h_2 & m_3 + h_3 & 1 \\ 0 & m_0 + h_0 & m_1 + h_1 & m_2 + h_2 \\ 0 & 0 & 0 & m_0 + h_0 \end{vmatrix} > 0.
 \end{aligned} \right.$$

Then the following result can be concluded.

Lemma 3.1. *If the condition (\mathbf{H}_2) holds, then the positive endemic equilibrium point E^\star is locally asymptotically stable in the absence of time-delay.*

We now discuss the case of positive delay, i.e, $\tau > 0$. Let $\lambda = i\omega$ ($\omega > 0$) be a root of (3.3), then by substituting it into (3.3) and separating the real and imaginary parts, we can obtain

$$\begin{cases} (h_1\omega - h_3\omega^3) \sin(\omega\tau) + (h_0 - h_2\omega^2) \cos(\omega\tau) = -\omega^4 + m_2\omega^2 - m_0, \\ (h_1\omega - h_3\omega^3) \cos(\omega\tau) - (h_0 - h_2\omega^2) \sin(\omega\tau) = m_3\omega^3 - m_1\omega. \end{cases} \quad (3.5)$$

By (3.5), the following equation can be acquired:

$$\omega^8 + G_{13}\omega^6 + G_{12}\omega^4 + G_{11}\omega^2 + G_{10} = 0, \quad (3.6)$$

where

$$\begin{aligned} G_{13} &= m_3^2 - h_3^2 - 2m_2, & G_{12} &= m_2^2 - h_2^2 - 2m_1m_3 + 2h_1h_3 + 2m_0, \\ G_{11} &= m_1^2 - h_1^2 - 2m_2m_0 + 2h_2h_0, & G_{10} &= m_0^2 + h_0^2. \end{aligned}$$

Suppose that $\xi = \omega^2$. Then (3.6) takes the form

$$P(\xi) = \xi^4 + G_{13}\xi^3 + G_{12}\xi^2 + G_{11}\xi + G_{10} = 0. \quad (3.7)$$

Lemma 3.2. *For the distribution of roots of (3.7), we set*

$$\begin{aligned} r_1 &= \frac{1}{2}G_{12} - \frac{3}{16}G_{13}^2, & r_2 &= \frac{1}{32}G_{13}^3 - \frac{1}{8}G_{13}G_{12} + G_{11}, \\ \Omega_1 &= \left(\frac{r_2}{2}\right)^2 + \left(\frac{r_1}{3}\right)^3, & \Omega_2 &= \frac{-1 + i\sqrt{3}}{2} \\ y_1 &= \sqrt[3]{-\frac{r_2}{2} + \sqrt{\Omega_1}} + \sqrt[3]{-\frac{r_2}{2} - \sqrt{\Omega_1}}, \\ y_2 &= \sqrt[3]{-\frac{r_2}{2} + \sqrt{\Omega_1}\Omega_2} + \sqrt[3]{-\frac{r_2}{2} - \sqrt{\Omega_1}\Omega_2^2}, \\ y_3 &= \sqrt[3]{-\frac{r_2}{2} + \sqrt{\Omega_1}\Omega_2^2} + \sqrt[3]{-\frac{r_2}{2} - \sqrt{\Omega_1}\Omega_2}, & \xi_i &= y_i - \frac{3G_{13}}{4}, \quad (i = 1, 2, 3). \end{aligned}$$

Then for (3.7), we have:

- (i) If $G_{10} < 0$, then (3.7) has at least one positive root.
- (ii) If $G_{10} \geq 0$ and $\Omega_1 \geq 0$, then (3.7) has positive roots if and only if $\xi_1 > 0$ and $P(\xi_1) < 0$.
- (iii) If $G_{10} \geq 0$ and $\Omega_1 < 0$, then (3.7) has positive roots if and only if there exists at least one $\xi^* \in (\xi_1, \xi_2, \xi_3)$, such that $\xi^* > 0$ and $P(\xi^*) \leq 0$.

By using of (3.2), we can get the corresponding threshold value $\tau_k > 0$ as follows:

$$\tau_k = \frac{1}{\omega} \left[\arccos \left(\frac{A_3\omega^6 + A_2\omega^4 + A_1\omega^2 + A_0}{B_3\omega^6 + B_2\omega^4 + B_1\omega^2 + B_0} \right) + 2k\pi \right], \quad (k = 0, 1, 2, \dots), \quad (3.8)$$

where

$$\begin{aligned}
 A_3 &= h_2 - m_3h_3, & A_2 &= m_3h_1 - m_2h_2 - m_1h_3 - h_0, \\
 A_1 &= m_2h_0 - m_1h_1 + m_0h_2, & A_0 &= -m_0h_0, & B_3 &= h_3^2, & B_2 &= h_2^2 - 2h_1h_3, \\
 B_1 &= h_1^2 - 2h_2h_0, & B_0 &= h_0^2.
 \end{aligned}$$

Hence, the corresponding bifurcation point can be defined as

$$\tau_0 = \min\{\tau_k\}.$$

To verify the transversality condition for occurrence of a Hopf bifurcation, let $\lambda(\tau) = \varphi_1(\tau) + i\omega(\tau)$ be a root of (3.3). Then $\varphi_1(\tau_k) = 0$ and $\omega(\tau_k) = \omega_0$ when $\tau = \tau_k$.

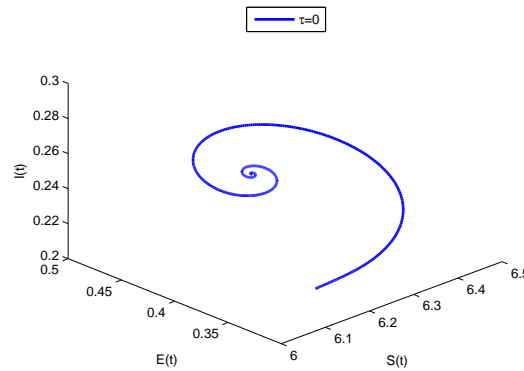


FIGURE 2. The phase portrait of model (1.2) in the absence of time-delay.

Lemma 3.3. Assume that $P'(\xi_k) \neq 0$, ($k = 1, 2, 3$). Then

$$\frac{d(\text{Re}\lambda(\tau_k))}{d\tau} \neq 0 \quad \text{and} \quad \text{sign} \left[\frac{d(\text{Re}\lambda(\tau_k))}{d\tau} \right] = \text{sign} [P'(\xi_k)].$$

Proof. It is obvious that when $\tau > \tau_k$, then there exists at least one eigenvalue with positive real part. By differentiating the two sides of Eq. (3.3) with respect to τ , we can obtain

$$\begin{aligned}
 & \left[4\lambda^3 + 3m_3\lambda^2 + 2m_2\lambda + m_1 + (3h_3\lambda^2 + 2h_2\lambda + h_1)e^{-\lambda\tau} - (h_3\lambda^3 + h_2\lambda^2 \right. \\
 & \left. + h_1\lambda + h_0)\tau e^{-\lambda\tau} \right] \frac{d\lambda}{d\tau} = (h_3\lambda^3 + h_2\lambda^2 + h_1\lambda + h_0)\lambda e^{-\lambda\tau}.
 \end{aligned}$$

This gives

$$\begin{aligned} \left(\frac{d\lambda}{d\tau}\right)^{-1} &= \frac{(3h_3\lambda^2 + 2h_2\lambda + h_1)e^{-\lambda\tau} - (h_3\lambda^3 + h_2\lambda^2 + h_1\lambda + h_0)\tau e^{-\lambda\tau}}{\lambda(h_3\lambda^3 + h_2\lambda^2 + h_1\lambda + h_0)e^{-\lambda\tau}} \\ &\quad + \frac{(4\lambda^3 + 3m_3\lambda^2 + 2m_2\lambda + m_1)}{\lambda(h_3\lambda^3 + h_2\lambda^2 + h_1\lambda + h_0)e^{-\lambda\tau}} \\ &= \frac{3h_3\lambda^2 + 2h_2\lambda + h_1 + (4\lambda^3 + 3m_3\lambda^2 + 2m_2\lambda + m_1)e^{\lambda\tau}}{\lambda(h_3\lambda^3 + h_2\lambda^2 + h_1\lambda + h_0)} - \frac{\tau}{\lambda}. \end{aligned}$$

Then it implies that

$$\begin{aligned} \text{sign} \left[\frac{d\text{Re}(\lambda)}{d\tau} \right]_{\tau=\tau_0, \lambda=i\omega_0} &= \text{sign} \left\{ \text{Re} \left(\frac{d\lambda}{d\tau} \right)^{-1} \right\}_{\tau=\tau_0, \lambda=i\omega_0} \\ &= \text{sign} \left\{ \text{Re} \left[\frac{3h_3\lambda^2 + 2h_2\lambda + h_1}{\lambda(h_3\lambda^3 + h_2\lambda^2 + h_1\lambda + h_0)} \right. \right. \\ &\quad \left. \left. + \frac{(4\lambda^3 + 3m_3\lambda^2 + 2m_2\lambda + m_1)e^{\lambda\tau}}{\lambda(h_3\lambda^3 + h_2\lambda^2 + h_1\lambda + h_0)} - \frac{\tau}{\lambda} \right] \right\}_{\tau=\tau_0, \lambda=i\omega_0} \\ &= \text{sign} \left\{ \text{Re} \left[\frac{(3h_3\omega_0^2 + 2h_2i\omega_0 + h_1)}{(h_3i\omega_0^3 + h_2\omega_0^2 + h_1i\omega_0 + h_0)i\omega_0} \right. \right. \\ &\quad \left. \left. + \frac{(4i\omega_0^3 + 3m_3\omega_0^2 + 2m_2i\omega_0 + m_1)(\cos(\omega_0\tau_0) + i\sin(\omega_0\tau_0))}{(h_3i\omega_0^3 + h_2\omega_0^2 + h_1i\omega_0 + h_0)i\omega_0} \right] \right\} \\ &= \text{sign} \left\{ \frac{1}{\Pi} \left[4\omega_0^6 + 3(m_3^2 - h_3^2 - 2m_2)\omega_0^4 + 2(m_2^2 - h_2^2 + 2h_1h_3 \right. \right. \\ &\quad \left. \left. - 2m_1m_3 + 2m_0)\omega_0^2 + m_1^2 - h_1^2 + 2h_0h_2 - 2m_0m_2 \right] \right\} \\ &= \text{sign} \left\{ \frac{1}{\Pi} (4\xi^3 + 3G_{13}\xi^2 + 2G_{12}\xi + G_{11}) \right\} = \text{sign} \left\{ \frac{1}{\Pi} (P'(\xi)) \right\}, \end{aligned}$$

where $\Pi = h_3^2\omega_0^6 + (h_2^2 - 2h_1h_3)\omega_0^4 + (h_1^2 - 2h_0h_2)\omega_0^2 + h_0^2$. It follows from the hypothesis (\mathbf{H}_3) that $P'(\xi) \neq 0$. Therefore the transversality condition

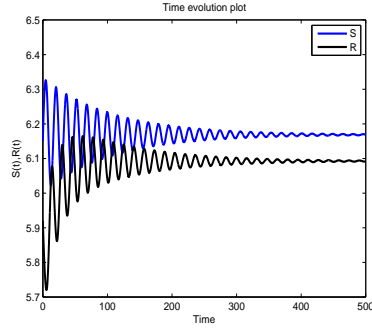
$$\left. \frac{d(\text{Re}(\lambda))}{d\tau} \right|_{\tau=\tau_0, \lambda=i\omega_0} \neq 0,$$

is satisfied which shows a Hopf bifurcation occurs at $\tau = \tau_0$. This completes the proof. \square

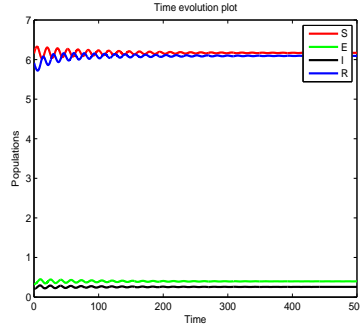
Hence, we now have the following conclusions.

Theorem 3.4. *Suppose that conditions (H_1) and (H_2) are satisfied. Then we have the following results:*

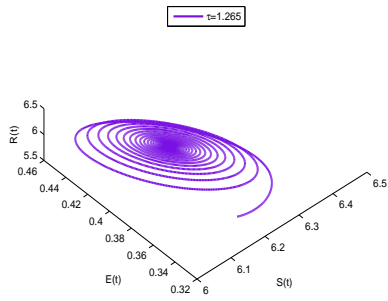
- (i) *If $0 \leq \tau < \tau_0$, then the endemic equilibrium $E^\star(S^\star, E^\star, I^\star, R^\star)$ of delayed model (1.2) is locally asymptotically stable. When $\tau > \tau_0$, the equilibrium point E^\star becomes unstable.*
- (ii) *When system (1.2) satisfies the transversality condition of lemma 3.3, the delayed model (1.2) undergoes a Hopf bifurcation at the positive equilibrium E^\star when time-delay $\tau = \tau_k$, where τ_k is defined by (3.8).*



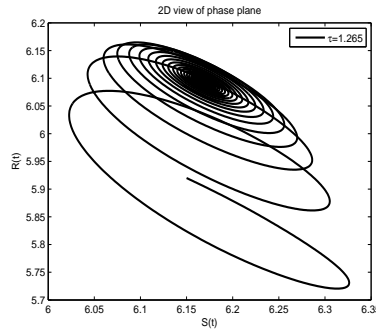
(a) $\tau = 1.265 < \tau_0 = 1.287$



(b) $\tau = 1.265 < \tau_0 = 1.287$



(c) $\tau = 1.265 < \tau_0 = 1.287$



(d) $\tau = 1.265 < \tau_0 = 1.287$

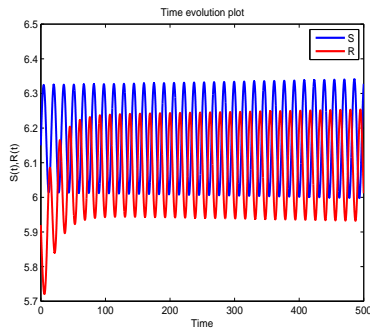
FIGURE 3. Effect of time-delay on the dynamics of delayed epidemic model (1.2).

4. NUMERICAL SIMULATIONS

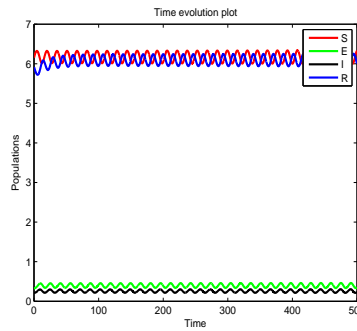
In this section, some numerical simulations are conducted to demonstrate the pandemic dynamics of COVID-19, and to verify the theoretical analysis of previous section. We consider a set of parameter values as in Table 2.

TABLE 2. Set of values for the original system’s parameters.

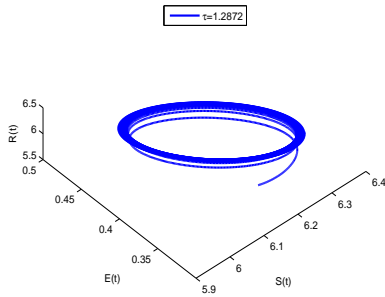
| Parameter | η | α | β | γ | ρ | δ | μ |
|-----------|--------|----------|---------|----------|--------|----------|-------|
| Value | 0.62 | 0.25 | 0.95 | 1.42 | 0.012 | 0.03 | 0.018 |



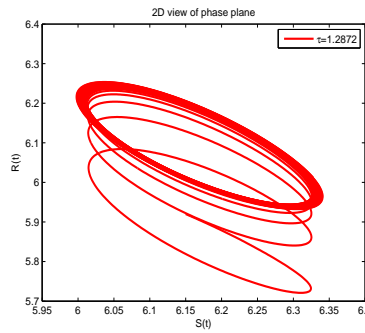
(a) $\tau = 1.2872 > \tau_0 = 1.287$



(b) $\tau = 1.2872 > \tau_0 = 1.287$



(c) $\tau = 1.2872 > \tau_0 = 1.287$



(d) $\tau = 1.2872 > \tau_0 = 1.287$

FIGURE 4. Time series and phase portraits of delayed epidemic model (1.2).

According to the parameters’ values of Table 2, the positive equilibrium point $E^\star(S^\star, E^\star, I^\star, R^\star)$ is calculated as

$$E^\star(6.16869, 0.39781, 0.25744, 6.09272).$$

When $\tau = 0$, the positive equilibrium point E^\star is asymptotically stable (see Figure 2). For $\tau > 0$, we can obtain $\omega_0 = 0.40521$ and $\tau_0 = 1.287$. Thus, when $\tau = 1.265 \in [0, \tau_0)$, the delayed system (1.2) has stable dynamics as are illustrated by Figure 3 and Figures 5(a) and 5(c). However, once the time-delay exceeds the threshold value, i.e, $\tau = 1.2872 > \tau_0 = 1.287$, E^\star loses its

stability and due to

$$\left[\frac{d(\operatorname{Re}\lambda(\tau))}{d\tau} \right]_{\tau=\tau_0}^{-1} \approx 1.24123 > 0, \quad \left[\frac{d(\operatorname{Re}\lambda(\tau))}{d\tau} \right]_{\tau=\tau_0} \approx 0.45665 > 0,$$

a Hopf bifurcation occurs (see Figure 4 and Figures 5(b) and 5(d)).

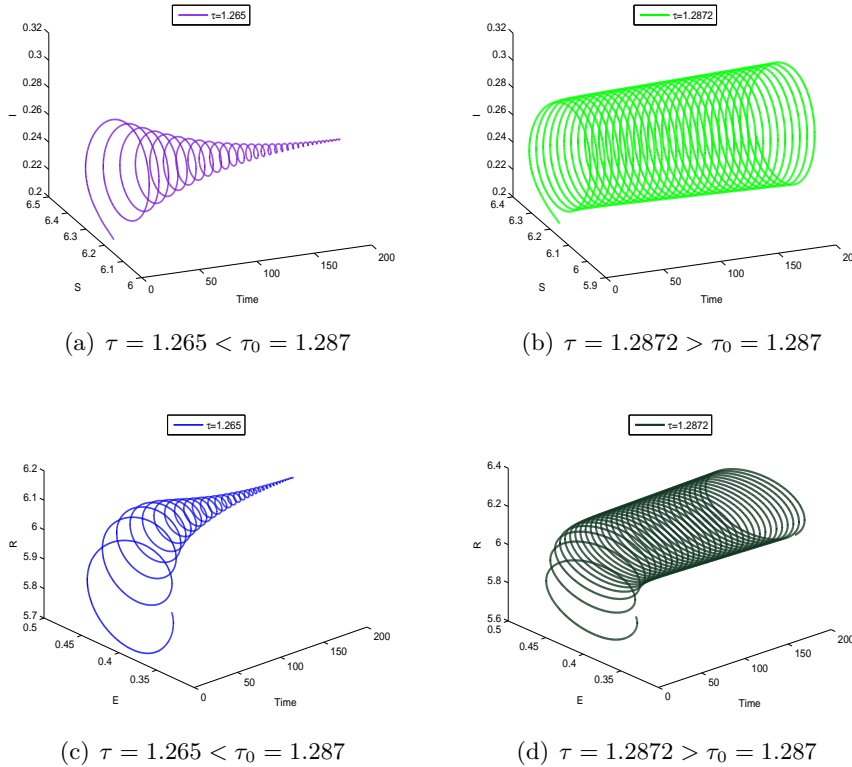


FIGURE 5. Various projection of the phase portraits of delayed epidemic model (1.2).

5. CONCLUSION

In this paper a SEIR delayed mathematical model describing the dynamics of COVID-19 is formulated and the effect of the time-delay on the dynamics of the model is investigated. It is found that existence of delay in the model leads to a local Hopf bifurcation and the model becomes unstable under some certain conditions. The obtained results show that when the delay parameter is suitable and small, the endemic equilibrium is asymptotically stable. In this case, the propagation of coronavirus can be predicted and controlled.

However, when the time-delay τ exceeds its critical value. Then the endemic equilibrium loses its stability and a Hopf bifurcation occurs which implies that the disease will be out of control.

REFERENCES

- [1] A. Abta, H. Laarabi, and H.T. Alaoui, Mathematical epidemiology model analysis on the dynamics of COVID-19 pandemic, *International Journal of Analysis*, (2014), 1–10.
- [2] S. M. Al-Tuwairqi, and S. K. Al-Harbi, A time-delayed model for the spread of COVID-19 with vaccination, *Scientific Reports*, **12** (2022), 19453.
- [3] A. F. Bezabih, G. K. Edessa, and P. R. Koya, Mathematical epidemiology model analysis on the dynamics of COVID-19 pandemic, *American Journal of Applied Mathematics*, **8** (5) (2020), 247–256.
- [4] O. Babasola, O. Kayode, and O.J. Peter, Time-delayed modelling of the COVID-19 dynamics with a convex incidence rate, *Informatics in Medicine Unlocked*, **35** (2022), 101124.
- [5] C. Balsa, I. Lopes, T. Guarda, and J. Rufno, Computational simulation of the COVID-19 epidemic with the SEIR stochastic model, *Computational and Mathematical Organization Theory*, (2021), 1–19.
- [6] S. Cakan, Dynamic analysis of a mathematical model with health care capacity for COVID-19 pandemic, *Chaos Solitons Fractals*, **139** (2020), 110033.
- [7] H. K. Ebraheem, N. Alkhateeb, H. Badran, and E. Sultan, Delayed dynamics of SIR model for COVID-19, *Open Journal of Modelling and Simulation*, **9** (2021), 146–158.
- [8] T. Erneux, J. Javaloyes, M. Wolfrum, and S. Yanchuk, Introduction to focus issue: Time-delay dynamics, *Chaos*, (27) (2017), 114201.
- [9] S. Gao, Z. Teng, and D. Xie, The effects of pulse vaccination on SEIR model with two time delays, *Appl. Math. Comput.*, **201** (2008), 282–292.
- [10] A. Khan, R. Ikram, A. Din, U. W. Humphries, and A. Akgul, Stochastic COVID-19 SEIQ epidemic model with time-delay, *Results in Physics*, **30** (2021), 104775.
- [11] H. Lu, Y. Ding, S. Gong, and S. Wang, Mathematical modeling and dynamic analysis of SIQR model with delay for pandemic COVID-19, *Math. Biosci. Eng.*, **18** (2021), 3197–3214.
- [12] A. Mahata, S. Paul, S., Mukherjee, and B. Roy, Stability analysis and Hopf bifurcation in fractional order SEIRV epidemic model with a time delay in infected individuals, *Partial Differential Equations in Applied Mathematics*, **5**(2022), 100282.
- [13] F. A. Rihan, H. J. Alsakaji, and C. Rajivganthi, Stochastic SIRC epidemic model with time-delay for COVID-19, *Advances in Difference Equations*, **502** (2020), 1–20.
- [14] A. Raza, A., Ahmadian, M. Rafiq, S. Salahshour, M. Naveed, M. Ferrara, and A.H. Soori, Modeling the effect of delay strategy on transmission dynamics of HIV/AIDS disease, *Advances in Difference Equations*, **663**(2020), 1–13.
- [15] M. Radha, and S. Balamuralitharan, A study on COVID-19 transmission dynamics: stability analysis of SEIR model with Hopf bifurcation for effect of time delay, *Advances in Difference Equations*, **523** (2020), 1–20.
- [16] R. Rakkiyappan, K. Udhayakumar, G. Velmurugan, J. Cao and A. Alsaedi, Stability and Hopf bifurcation analysis of fractional-order complex-valued neural

- networks with time delays, *Partial Differential Equations in Applied Mathematics*, **225** (2017), 1–25.
- [17] S. Tipsri, and W. Chinviriyasit, The effect of time delay on the dynamics of an SEIR model with nonlinear incidence, *Chaos Solitons Fractals*, **75** (2015), 153–172.
- [18] J. Wang, Mathematical models for COVID-19: applications, limitations, and potentials, *J Public Health Emerg.*, **4** (2020), 1–5.
- [19] Y. Wang, J. Cao, G. Q. Sun, and J. Li, Effect of time delay on pattern dynamics in a spatial epidemic model, *Physica A*, **412** (2014), 137–148.
- [20] W. Yang, Modeling COVID-19 pandemic with hierarchical quarantine and time delay, *Dynamic Games and Applications*, **(11)** (2021), 892–914.
- [21] P. Yan, and S. Liu, SEIR epidemic model with delay, *ANZIAM J.*, **48** (2006), 119–134.
- [22] H. M., Youssef, N. A. Alghamdi, M. A. Ezzat, A. A. El-Bary, and A. M. Shawky, A new dynamical modeling SEIR with global analysis applied to the real data of spreading COVID-19 in Saudi Arabia, *Mathematical Biosciences and Engineering*, **17 (6)** (2020), 7018–7044.
- [23] F. Yang, and Z. Zhang, A time-delay COVID-19 propagation model considering supply chain transmission and hierarchical quarantine rate, *Adv. Difer. Equ.*, **191** (2021), 1–21.
- [24] W. Yang, Modeling COVID-19 Pandemic with Hierarchical Quarantine and Time Delay, *Dynamic Games and Applications*, **11** (2021), 892–914.
- [25] F.-F. Zhang, Z. Jin, and G-Q. Sun, Bifurcation analysis of a delayed epidemic model, *Applied Mathematics and Computation* **(216)** (2010), 753–767.
- [26] M. A. Zaitri, C. J. Silva, and D. F. M. Torres, Stability Analysis of Delayed COVID-19 Models, *Axioms*, **11(400)** (2022), 1–21.